# Analysis of PDA dose curves for the extraction of antimicrobial peptide properties

*Jiangtao Zhao,[1] Kaori Sugihara[1,2]**

[1]Department of Physical Chemistry, University of Geneva, Quai Ernest Ansermet 30, 1211 Geneva 4, Switzerland

[2]Institute of Industrial Science, The University of Tokyo, 4-6-1 Komaba Meguro-Ku, Tokyo 153-8505, Japan

*email: kaori-s@iis.u-tokyo.ac.jp

**Keywords**

Polydiacetylene; Antimicrobial peptide; Cooperative effect

**Abstract**

A mechanochromic polymer, polydiacetylene, changes color upon ligand binding, being a popular material in biosensing. However, whether it can also detect ligand functions in addition to binding is left understudied. In this work, we report that the polydiacetylene can be used to determine the net charges and the mode of actions (carpet model, toroidal pore model etc.) of antimicrobial peptides and detergents via $EC_{50}$ and Hill coefficients from the colorimetric response dose curves. This opens a potential for a high-throughput peptide screening by functions, which is difficult with the conventional methods.

## Introduction

Polydiacetylene (PDA) is a mechanochromic polymer that switches its color from blue to red and emits fluorescence when it is stimulated by external perturbations[1-2]. Significant efforts have been made in the past decades to develop PDA colorimetric sensors for the detection of temperature[3-6], pH[7-8], ions[9-10], mechanical stresses[11-13], ligands[14], antibodies[15], aptamers[16-17] etc. For the recognition of a specific molecule, often the headgroup of the PDA is functionalized, so that it specifically binds to the ligand of interest. After the calibration of the colorimetric response against the concentration of the ligand in solution, PDA can be used as a colorimetric binding assay[18-19].

In contrast, Jelinek group has discovered that different kinds of antimicrobial peptides stimulate PDAs embedded in phospholipid bilayers at a various level in the absence of such a specific interaction[20-21]. This indicates that the PDA color reflects the nature of the lipid-peptide interactions, opening a potential use of PDA as a functional assay. This work has been further expanded towards the membrane interaction/penetration assay for drug screening, where the colorimetric dose curves were categorized and linked to the mode of action of drugs[22]. Being inspired by these works, recently, we have shown that the PDA peptide chromism is linked to the solid-to-liquid phase transition of the diacetylene monomers[23-24].

In this work, to find which peptide functional parameters can be extracted by the PDA color change, we analyzed the colorimetric dose curves of PDA vesicles made of 10,12-tricosadiynoic acid (TRCDA) and 1,2-dioleoylsn-glycero-3-phosphocholine (DOPC) for different types of antimicrobial peptides and detergents. This systematic study revealed that $EC_{50}$ (the ligand concentration producing the median effect of 50%) was correlated to their net charge and the Hill coefficient (a parameter that represents the steepness of the curve and is associated with the cooperativity of the ligand) was linked to the model of the peptide-lipid interactions (e.g. carpet model, toroidal pore model). This suggests a potential of PDA as a facile colorimetric assay to screen peptides for their electric charges or by functions. In addition, we will also show a proof-of-principle of an antimicrobial peptide cooperative effect (synergy or antagonism) detection by PDA.

## Materials and methods

For a detailed summary of the materials and methods used in this study, see Supporting Information.

## Results and discussions

**Dose curves from the colorimetric response were obtained against 7 peptides and detergents.** To compare the PDA chromism stimulated by different types of peptides and detergents, PDA suspension made of 75% TRCDA + 25% DOPC was incubated with LL-37, melittin, PGLa, Magainin 2, IAPP, $C_{12}E_8$ and CHAPS at different concentrations and their UV-VIS spectra were measured (Figure 1a, b). DOPC was added to form homogenous vesicle suspension and to improve the sensitivity towards antimicrobial peptides and detergents[20, 23, 25-26]. Colorimetric response (C.R.), which is the quantification of the PDA color by taking the intensity ratio between the blue peak at 645 nm and the red peak at 545 nm, commonly used for the PDA analysis, was extracted from these spectra and plotted against the peptide concentrations (Figure 1c). Each molecule yielded a different dose curve as it reflects its unique interaction with PDA. The potency is the highest for LL37, whereas CHAPS is especially low. In addition, the shape of the dose curves also varies from molecules to molecules. To understand these details quantitatively, EC50 and Hill coefficients were extracted from these dose curves (Figure 2a, b).

**$EC_{50}$ exponentially decays with the peptides' net charge.** First, we found that $EC_{50}$ is inversely correlated with the peptides' net charge (Figure 2a). The binding mechanism between lipids and antimicrobial peptides has been extensively studied before and has been mainly explained by the combination of the Gouy-Chapman theory (concentration of peptides immediately above the membrane surface due to the electrostatic attraction between the peptides and the membrane) and the partition equilibrium. Antimicrobial peptides are generally cationic, thus attracted to the anionic carboxyl headgroups of PDA (net charge -1 per monomer), elevating their local concentration right above the PDA surface. This concentration right above the PDA surface $c_M$ can be expressed by the following equation[27].

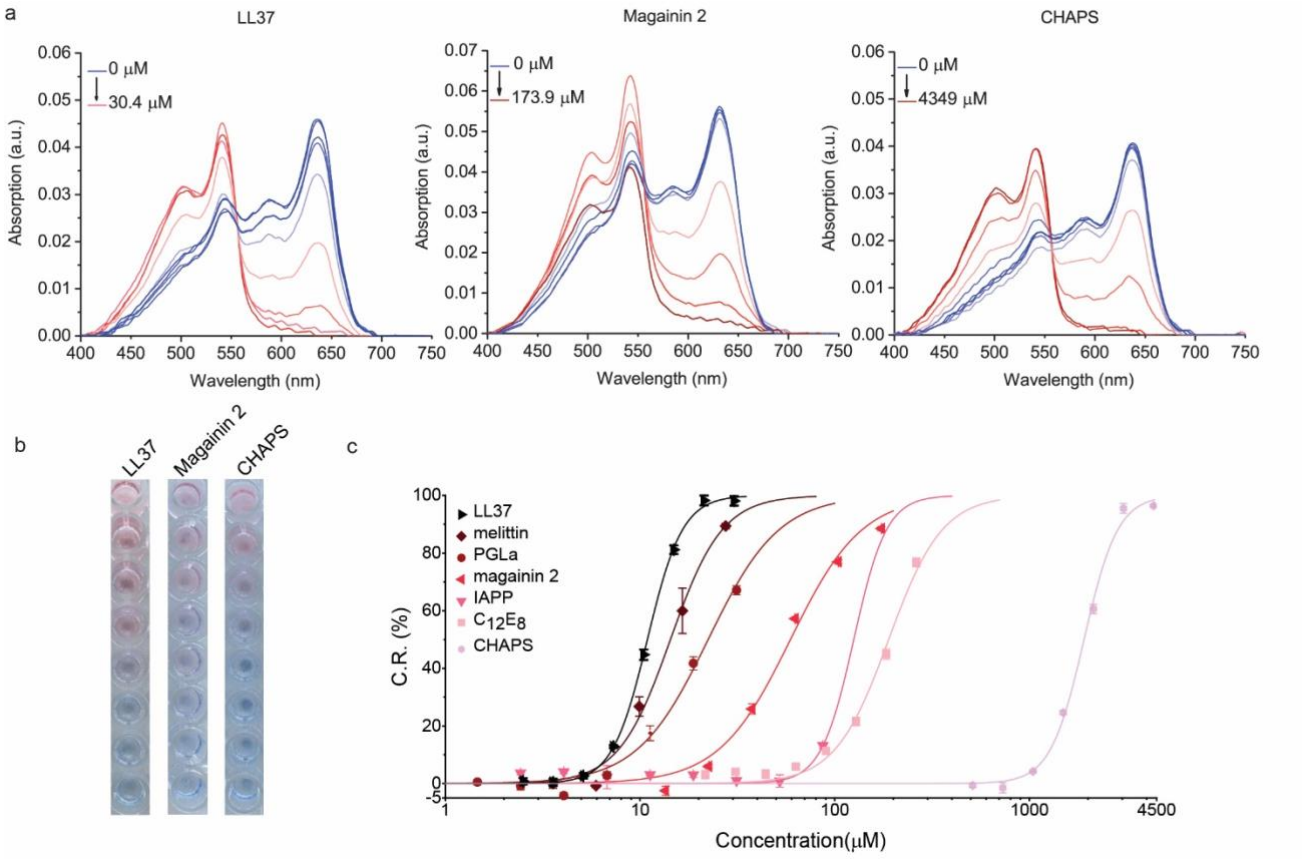


Figure 1: a, UV-VIS spectra of PDA suspension made of 75% TRCDA + 25% DOPC in HEPES buffer solution (150 mM NaCl, pH7.4) when LL-37, Magainin 2, and CHAPS were added at different concentrations. b, Photographs of these PDA suspensions. Note that the concentrations in each well correspond to the ones indicated in (a). c, Colorimetric response (C.R.) calculated from these UV-VIS spectra plotted against the peptide concentrations.

$$c_{\mathrm{M}} = c_{\mathrm{f}} e^{-zF_0\psi_0/RT}, \qquad \text{(eq. 1)}$$

where $c_{\mathrm{f}}$ is the peptide concentration in bulk solution, $z$ is the peptide charge, $F_0$ is the Faraday constant, $\psi_0$ is the surface potential linked to the membrane charge density, $R$ is the gas constant, and $T$ is the temperature. When a negatively charged bilayer ($\psi_0 < 0$) is incubated with peptides at a fixed bulk concentration $c_{\mathrm{f}}$ at $T$, the peptide concentration right above the bilayer $c_{\mathrm{M}}$ exponentially grows as a function of the peptides' net charge $z$ (> 0). This explains why elevating $z$ shifts $EC_{50}$ towards lower concentrations, because it increases $c_{\mathrm{M}}$, making the molecule more potent. This argument assumes that the equilibrium constants between bilayers and peptides at nanoscale are in the same order of magnitude for all the tested molecules, whereas the intrinsic affinity is predominantly governed by $z$. By fitting the data in Figure 2a with the following eq. 1' (eq. 1 solved for $c_{\mathrm{f}}$)

$$c_{\mathrm{f}} = c_{\mathrm{M}} e^{zF_0\psi_0/RT}, \qquad \text{(eq. 1')}$$

where $c_{\mathrm{f}}$ ($EC_{50}$ in $y$ axis) and $z$ (net charge in $x$ axis) are the variables, $R$ = 8.31 $JK^{-1}mol^{-1}$, $T$ = 293 K, $F_0$ = 9.65 x $10^4$ $Cmol^{-1}$ are the constants, $c_{\mathrm{M}}$ and $\psi_0$ are the open parameters, we obtain $c_{\mathrm{M}}$ = 1058 ± 10 μM and $\psi_0$ = - 26 ± 1 mV (see Figure S1 for the details). The order of magnitude of this surface potential value is reasonable for bilayers made of a mixture of TRCDA (net charge -1) and DOPC (net charge 0) as the one estimated for 100% POPS (1-palmitoyl-2-oleoyl-sn-glycero-3-phospho-L-serine) bilayers (net charge -1) has been reported as - 103 ~ -158 mV[28-29]. This implies that the above-mentioned assumption is probably correct, where the intrinsic affinity of peptides to bilayers is mainly governed by $z$, although other factors such as a difference in the hydrophobicity in each peptide also plays a role in details[30]. Previously in an effort to study the membrane affinity of drugs with PDA, Wei and coworkers have shown that log($EC_{50}$) extracted from PDA dose curves and the intrinsic partition coefficient log(Km) present a linear correlation.[31] In another study, Katz and coworkers have shown a link between the drug-membrane interactions and $EC_{50}$ of PDA dose curves[22]. These previous works also

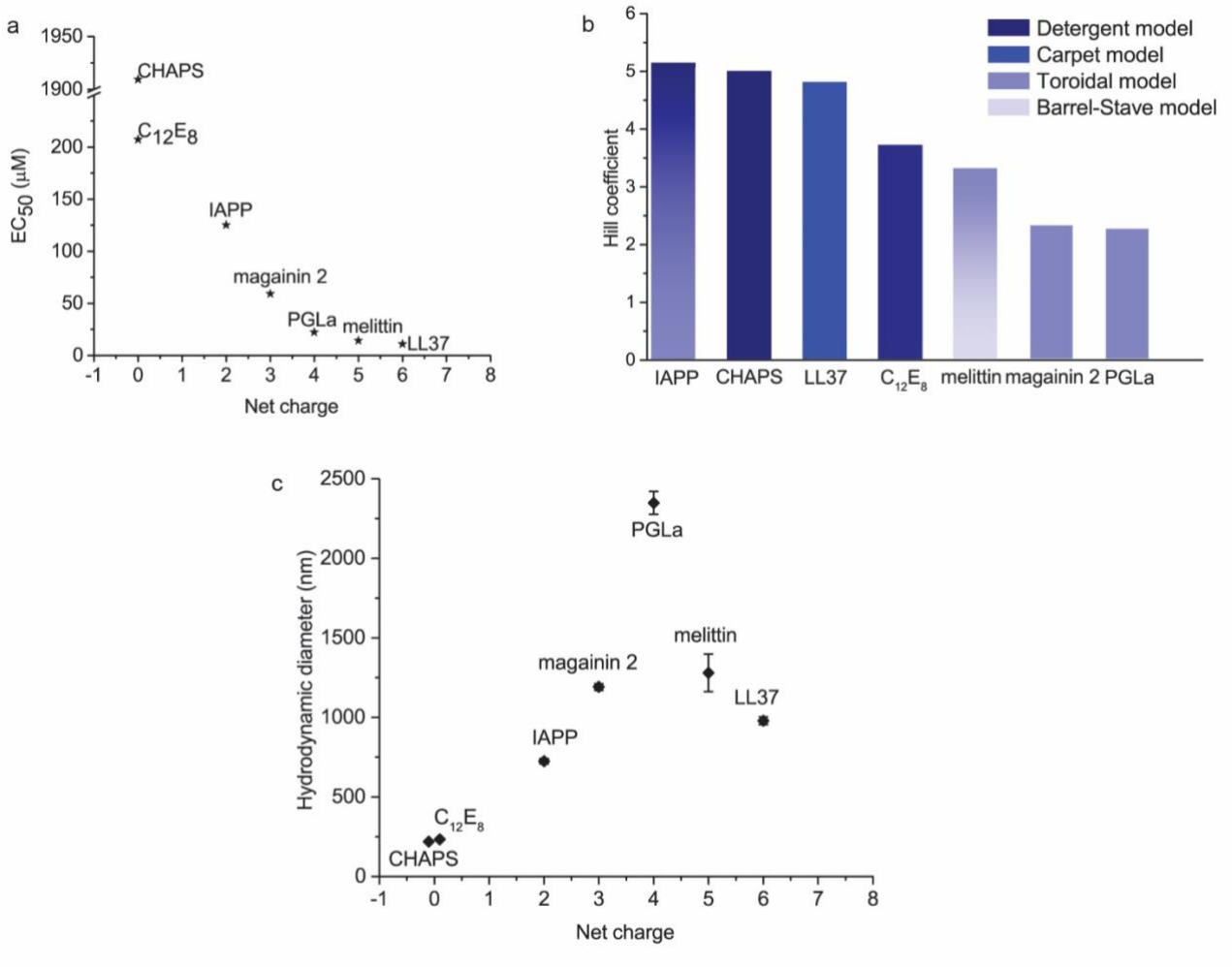


Figure 2: $EC_{50}$ (a) and Hill coefficients (b) were extracted from the dose curves in Fig. 1c and plotted against the net charge and the peptide types respectively. Note that the Hill coefficient (5.16) extracted from the dose curve of IAPP is a rough estimate due to the lack of data points in higher concentrations. c, The particle size estimated by dynamic light scattering (DLS) at $EC_{50}$ induced by peptides or detergents.

support that PDA color change well corresponds to the affinity of the molecules.

**Hill coefficients are linked to the mode of action of each molecule.** Hill coefficient reflects the slope of the dose curves and is a parameter used to describe the cooperativity of ligand-receptor binding. $n > 1$ and $n < 1$ suggest positive and negative cooperativity[32-33], respectively. Antimicrobial peptides and detergents are known to have such a cooperativity, where their oligomerization in membranes initiates a certain function such as pore formation[34] or bilayer destruction[35]. The strength of the cooperativity depends on their mode of action. For example, a peptide that forms a pore as a monomer is expected to have no cooperativity in its function, whereas the one that forms a pore as an oligomer via the barrel-stave or the toroidal model is expected to have a higher cooperativity. The ones that destroy membranes via the carpet model or the detergent model, where many peptides self-assemble into peptide-lipid complexes, are expected to have even higher cooperativity as the number of peptides that are involved in their functions is larger. Therefore, we hypothesized that the Hill coefficients extracted from the C.R. dose curves may be connected to the mode of action of each peptide. To study this hypothesis, first we summarize the known functions of each peptide and detergent in following. Magainin 2 and PGLa, isolated from the skin of African frog *Xenopus laevis*, are a well-known couple that exhibit a broad spectrum of antimicrobial activity. Both peptides adopt toroidal model in various compositions of phospholipid bilayers as evidenced by x-ray scattering[36] and $^{31}P$ and $^{2}H$ solid-state NMR spectroscopy[37]. Melittin is the main component of honeybee venom. Although its mode of action is still under debate, toroidal model and barrel-stave model are the two main proposed models.

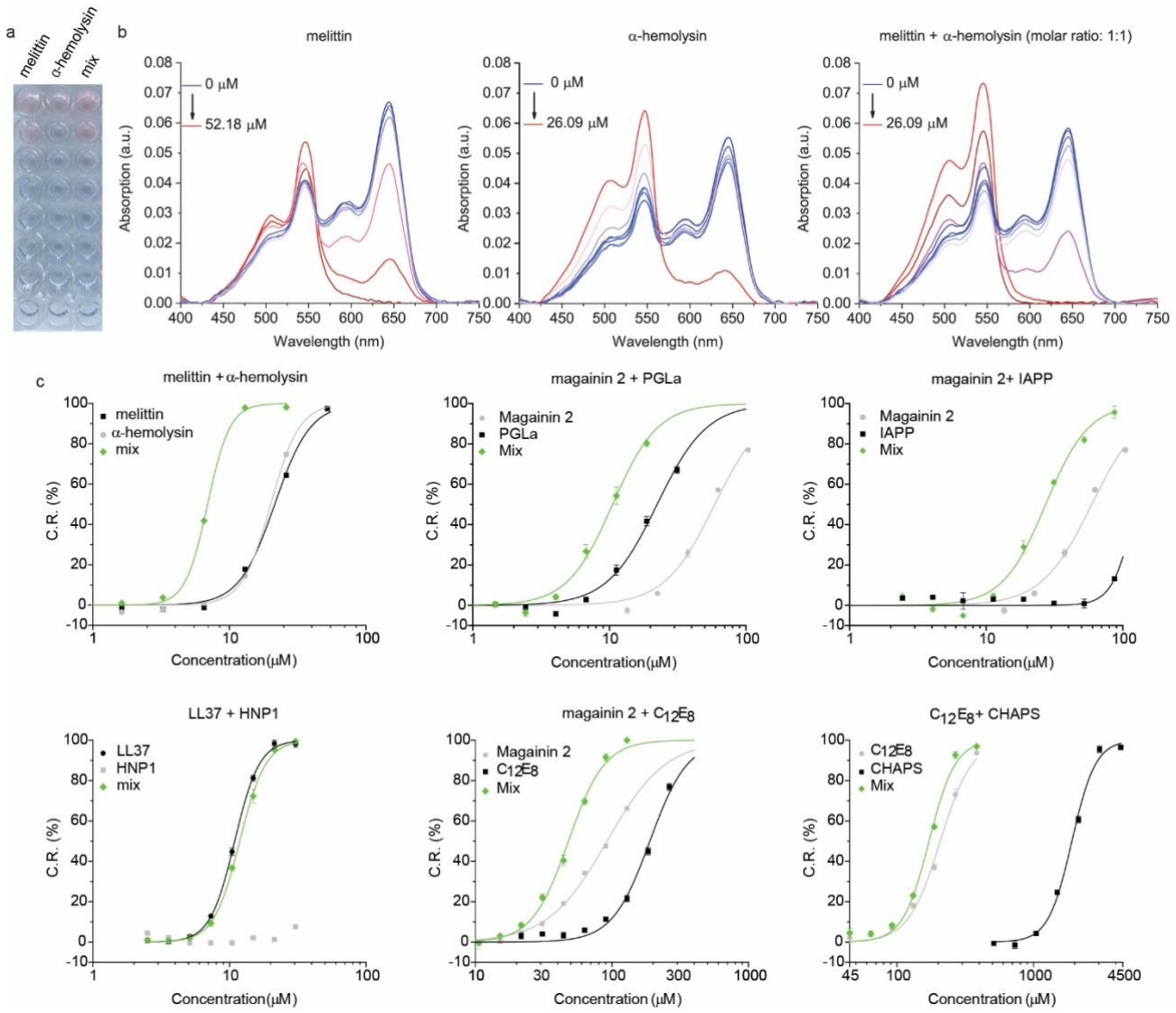


Figure 3: (a) Photographs and (b) UV-VIS spectra of PDA suspension made of 75% TRCDA + 25% DOPC in HEPES buffer solution (150 mM NaCl, pH7.4) when melittin, α-hemolysin and their mixture were added at different concentrations. c, Dose-effect curves of different couples of peptides and detergents.

Toroidal model has been supported by neutron scattering[38] and transmission electron microscopy[39]. Barrel-stave model has been supported by Raman spectroscopy[40] and solid-state $^{31}P$ and $^{13}C$ NMR[38, 41]. LL37, the only cathelicidin-derived peptide found in humans, has been reported to adopt the carpet-like mechanism by various methods. For example, a characteristic peak shifting in $^{31}P$ solid-state NMR[42] and the dichroic ratio $R^{ATR}$ and the lipid-order parameter $f$ calculated from attenuated total reflectance Fourier-transform infrared spectroscopy[43-44] have both indicated that LL-37 is surface localized and does not penetrate into the hydrophobic core of the membrane, which is compatible with the carpet model. Human islet amyloid polypeptide (IAPP) is known to form defects in membranes and induces cell death in amyloidosis. It has different aggregation stages such as low and high-number oligomers, protofibrils up to amyloid fibrils, where each aggregation state presents unique interaction with membranes. Oligomeric states seem to form toroidal pores, supported by an asymmetrically pyrene-labeled vesicle assay[45], differential scanning calorimetry (DSC) and solid-state NMR[46-47], whereas amyloid fibrils destroy membranes by creating a larger defects. In our experiment, we do not know the aggregation stage of IAPP, thus the mode of action can be anything between toroidal model to membrane destruction by amyloid fibril. $C_{12}E_8$ and CHAPS are two kinds of detergents that destroy membranes by micellization, which is called detergent model. Size and shape of the formed micelles caused by CHAPS have been investigated by small-angle x-ray scattering[48] and molecular dynamics simulations[49], whereas that of $C_{12}E_8$ have been studied by $^{2}H$ and $^{31}P$ NMR[50].

Table 1: Comparison of our results and the literatures. Calculated synergistic factor is indicated in parenthesis. The error bars in the combination index originates from the used C.R. value for the analysis (see Figure S2). Used lipids in the experiments reported in the literature is also indicated in parenthesis.

| Peptide couples | Our results | Literature |
|---|---|---|
| **Melittin + α-hemolysin** | Synergy (0.67±0.04) | - |
| **Magainin 2 + PGLa** | Synergy (0.65±0.02) | Synergy (BBPS)[51] |
| **Magainin 2 + IAPP** | Synergy (0.68±0.01) | Synergy (DOPG)[52] |
| **CHAPS + $C_{12}E_8$** | Synergy (0.92±0.02) | Synergy (POPC)[53] |
| **Magainin 2 + $C_{12}E_8$** | Synergy (0.78±0.07) | Additivity (POPC, POPG)[53] |
| **LL37 + HNP1** | Antagonism (1.09±0.01) | Antagonism (POPC)[54] |

The comparison between Hill coefficients obtained in our experiment and the known function of peptide/detergent shows that Hill coefficients and the peptide functions are in a good correlation as expected (Figure 2b). Molecules with higher Hill coefficients are mainly linked to the detergent or the carpet model, whereas the ones with lower Hill coefficients are correlated with the toroidal or the barrel-stave model. This implies that PDA can be used as a functional assay to screen peptides' mode of action in a high throughput manner.

**Dynamic light scattering shows net-charge dependent aggregation.** To study the aggregation behavior after mixing PDA and peptides, the samples were characterized by dynamic light scattering (DLS). The hydrodynamic diameter of TRCDA vesicles were 222 ± 3 nm and 274 ± 8 nm before and after polymerization, respectively. When peptides and detergents were added at each $EC_{50}$, the hydrodynamic diameter changed into 219 ± 2 nm, 233 ± 2 nm, 724 ± 17 nm, 1191 ± 20 nm, 2349 ± 72 nm, 1280 ± 118 nm, and 979 ± 24 nm for CHAPS, $C_{12}E_8$, IAPP, magainin, PGLa, melittin, and LL37, respectively (Figure 2c). First, the reason for the lack of aggregation for CHAPS and $C_{12}E_8$ is due to their zero net charge. As the net positive charge of the molecule increases, the aggregation was induced because their positive charges help with bridging negatively charged PDAs for forming large complexes. However, the aggregation peaks at PGLa (+4) and declines for melittin (+5) and LL37 (+6). This may be because their attachment to PDA inversed the PDA's zeta potential into positive, which rather counteracted the aggregation by electrostatic repulsion. $EC_{50}$ changed monotonically against the net charge (Figure 2a) in contrast to the aggregation (Figure 2c). This suggests that $EC_{50}$ managed to capture the charge of the molecules despite the different aggregation levels in the samples.

**PDA assay indicated a predictability for the peptide synergistic effects.** Next, we studied the PDA dose curves, where two types of peptides (detergents) are mixed at 1:1 molar ratio for an attempt to detect synergistic (cooperative) effects. Cooperative effects or synergy among antimicrobial peptides[55-73], where mixing different types of peptides boosts their antimicrobial efficiency, has garnered attention as a possible approach to improve their potency especially in the context of antibiotic resistance and because of its underlying interesting mechanism. In some cases, two kinds of peptides seem to interact in membranes, either enhancing or suppressing their ability to destroy bilayers, thus modulating their toxicity[54, 56, 74-79]. However, only several couples have been discovered to present such an interesting effect due to a lack of high-throughput methods to screen cooperative functions of peptides in bilayers. As a first step to investigate whether the PDA assay can be used for the cooperative function screening, we measured PDA dose curves from 6 peptide (detergent) couples; melittin + α-hemolysin, magainin 2 + PGLa, magainin 2 + IAPP, magainin 2 + $C_{12}E_8$, $C_{12}E_8$ + CHAPS, LL37 + HNP1 (Figure 3a-c), and their combination index were analysed (see SI). In brief, the combination index method analyses dose curves from individual compounds and that from their mixture for clarifying whether the effect from the mixture presents synergy (combination index < 1), antagonism (combination index > 1), or just an additive effect (combination index = 1), often used to evaluate combination therapies[80-81]. These couples were selected as their cooperative effects

have been previously investigated by vesicle leakage assays and the results have been reported in the literatures. For example, magainin 2 and PGLa have cooperatively induced a leakage of calcein from bovine brain phosphatidylserine (BBPS) vesicles[51]; The mixture of IAPP and magainin 2 has led to a leakage of fluorescent dextrans from DOPG vesicles and the inhibition of bacterial growth[52]; CHAPS and $C_{12}E_8$ have exhibited a synergistic activity of calcein leakage in POPC vesicles[53]; On the other hand, the mixture of magainin 2 and $C_{12}E_8$ has shown just an additive membrane permeabilization, studied by calcein leakage from POPC+POPG vesicles[53]; LL37 and HNP1 have antagonistically minimized cytotoxicity by protecting membranes from lysis, studied by fluorescence recovery after photobleaching (FRAP) with POPC bilayers and by cytotoxicity studies with eukaryotic cells[54].

The extracted combination index from the analysis is shown in Table 1 together with their known cooperative functions from the literatures. The result from the PDA assay has a moderate matching with the one from the literature. Especially, the fact that the activity of the rare antagonistic couple (LL37 + HNP1)[54] was recapitulated by the PDA assay is noteworthy. Magainin 2 + $C_{12}E_8$ were predicted as synergy in the PDA assay, whereas they have been reported to show additivity in the literature. This suggests the limitation of the PDA functional assay, where what the PDA color change reflects is not exactly the same as the function that is captured by vesicle leakage assays. In addition, for the magainin 2 + $C_{12}E_8$ couple, the Hill coefficient of their mixture (3.28) became rather close to that of $C_{12}E_8$ (3.15) than magainin (2.02), which is also visible by looking at the slopes of the dose curves in Figure 3c. Based on our observation that the Hill coefficient is linked to the mode of action, this may suggest that their combined function is similar to that of $C_{12}E_8$, although further studies are required for the confirmation.

## Conclusions

In conclusion, we found that $EC_{50}$ and Hill coefficient from PDA dose curves, when PDA is incubated with antimicrobial peptides or detergents, are linked to their net electric charge and bilayer interaction mechanism, respectively. EC50 and Hill coefficient are the two key parameters that identify dose curves and are often used for the analysis of high-throughput assays. Conventionally, the experimental determination of net charges or mode of actions of antimicrobial peptides typically requires much cumbersome techniques such as zeta-potential measurements, isothermal titration calorimetry, circular dichroism, vesicle leakage assays, or membrane conductance measurements, which consumes lots of expensive peptides and could take a few months to obtain data. In comparison, the presented colorimetric PDA assay was performed with the standard plate reader that enables an automatic acquisition of 96 spectra (with 96 well plate), opening a potential for high-throughput peptide screening by electric charges and functions.

## Acknowledgements

The research leading to these results has partly received funding from Swiss National Foundation, the Swiss National Centre of Competence in Research (NCCR) Chemical Biology, Foundation Ernst et Lucie Schmidheiny and Leading House for the Middle East and North Africa (University of Applied Sciences and Arts Western Switzerland), Shiseido Female Researcher Science Grant, UTEC-UTokyo FSI Research Grant Program, the FY 2020 University of Tokyo Excellent Young Researcher, Japan Society for the Promotion of Science (JP20K22324), Takeda Foundation, the Mitsubishi Foundation, Inoue Foundation for Science, the Naito Foundation and the Kanamori Foundation. We thank Dimitri Moreau and Kye Robinson for the access of the plate reader and DLS. J. Z. acknowledges the support from China Scholarship Council (CSC).

## Supporting information

Supporting figures (Figure S1, S2) and Materials and Methods are provided in Supplementary Information.

## References

1. Chance, R. R., Chromism in Polydiacetylene Solutions and Crystals. *Macromolecules* **1980,** *13* (2), 396-398.

2. Wegner, G. J. Z. N., Topochemische Reakionen von Monomeren mit Konjugierten Dreifachbindungen I. Mit.: Polymerisation von Derivaten des 2.4-Hexadiin-1.6-diols im Kristallinen Zustand. **1969,** *24*, 824-832.

3. Chance, R. R.; Patel, G. N.; Witt, J. D., Thermal effects on the optical properties of single crystals and solution - cast films of urethane substituted polydiacetylenes. *The Journal of Chemical Physics* **1979,** *71* (1), 206-211.
4. Chae, S.; Lee, J. P.; Kim, J.-M., Mechanically Drawable Thermochromic and Mechanothermochromic Polydiacetylene Sensors. *Advanced Functional Materials* **2016,** *26* (11), 1769-1776.
5. Girard-Reydet, C.; Ortuso, R. D.; Tsemperouli, M.; Sugihara, K., Combined Electrical and Optical Characterization of Polydiacetylene. *J Phys Chem B* **2016,** *120* (14), 3511-5.
6. Ortuso, R. D.; Ricardi, N.; Burgi, T.; Wesolowski, T. A.; Sugihara, K., The deconvolution analysis of ATR-FTIR spectra of diacetylene during UV exposure. *Spectrochim. Acta. A. Mol. Biomol. Spectrosc.* **2019,** *219*, 23-32.
7. Jannah, F.; Kim, J.-M., pH-sensitive colorimetric polydiacetylene vesicles for urease sensing. *Dyes and Pigments* **2019,** *169*, 15-21.
8. Yapor, J. P.; Alharby, A.; Gentry-Weeks, C.; Reynolds, M. M.; Alam, A. K. M. M.; Li, Y. V., Polydiacetylene Nanofiber Composites as a Colorimetric Sensor Responding To Escherichia coli and pH. *ACS Omega* **2017,** *2* (10), 7334-7342.
9. Xu, Q.; Lee, S.; Cho, Y.; Kim, M. H.; Bouffard, J.; Yoon, J., Polydiacetylene-Based Colorimetric and Fluorescent Chemosensor for the Detection of Carbon Dioxide. *Journal of the American Chemical Society* **2013,** *135* (47), 17751-17754.
10. Lee, K. M.; Chen, X.; Fang, W.; Kim, J.-M.; Yoon, J., A Dual Colorimetric and Fluorometric Sensor for Lead Ion Based on Conjugated Polydiacetylenes. *Macromolecular Rapid Communications* **2011,** *32* (6), 497-500.
11. Ortuso, R. D.; Sugihara, K., Detailed Study on the Failure of the Wedge Calibration Method at Nanonewton Setpoints for Friction Force Microscopy. *The Journal of Physical Chemistry C* **2018,** *122* (21), 11464-11474.
12. Park, D.-H.; Hong, J.; Park, I. S.; Lee, C. W.; Kim, J.-M., A Colorimetric Hydrocarbon Sensor Employing a Swelling-Induced Mechanochromic Polydiacetylene. *Advanced Functional Materials* **2014,** *24* (33), 5186-5193.
13. Juhasz, L.; Ortuso, R. D.; Sugihara, K., Quantitative and Anisotropic Mechanochromism of Polydiacetylene at Nanoscale. *Nano Letters* **2020,** *21* (1), 543-549.
14. Dolai, S.; Bhunia, S. K.; Beglaryan, S. S.; Kolusheva, S.; Zeiri, L.; Jelinek, R., Colorimetric Polydiacetylene–Aerogel Detector for Volatile Organic Compounds (VOCs). *ACS Applied Materials & Interfaces* **2017,** *9* (3), 2891-2898.
15. Lee, S. W.; Kang, C. D.; Yang, D. H.; Lee, J. S.; Kim, J. M.; Ahn, D. J.; Sim, S. J., The Development of a Generic Bioanalytical Matrix Using Polydiacetylenes. *Advanced Functional Materials* **2007,** *17* (13), 2038-2044.
16. Jung, S.-H.; Jang, H.; Lim, M.-C.; Kim, J.-H.; Shin, K.-S.; Kim, S. M.; Kim, H.-Y.; Kim, Y.-R.; Jeon, T.-J., Chromatic Biosensor for Detection of Phosphinothricin Acetyltransferase by Use of Polydiacetylene Vesicles Encapsulated within Automatically Generated Immunohydrogel Beads. *Analytical Chemistry* **2015,** *87* (4), 2072-2078.
17. Jung, Y. K.; Kim, T. W.; Park, H. G.; Soh, H. T., Specific Colorimetric Detection of Proteins Using Bidentate Aptamer-Conjugated Polydiacetylene (PDA) Liposomes. *Advanced Functional Materials* **2010,** *20* (18), 3092-3097.
18. Beasley, M.; Stonebraker, A. R.; Legleiter, J., Normalizing polydiacetylene colorimetric assays of vesicle binding across lipid systems. *Anal. Biochem.* **2020,** *609*.
19. Kim, T.; Moon, D.; Park, J. H.; Yang, H.; Cho, S.; Park, T. H.; Ahn, D. J., Visual detection of odorant geraniol enabled by integration of a human olfactory receptor into polydiacetylene/lipid nano-assembly. *Nanoscale* **2019,** *11* (16), 7582-7587.
20. Kolusheva, S.; Boyer, L.; Jelinek, R., A colorimetric assay for rapid screening of antimicrobial peptides. *Nature Biotechnology* **2000,** *18* (2), 225-227.
21. Kolusheva, S.; Shahal, T.; Jelinek, R., Peptide-membrane interactions studied by a new phospholipid/polydiacetylene colorimetric vesicle assay. *Biochemistry (Mosc).* **2000,** *39* (51), 15851-15859.
22. Katz, M.; Ben-Shlush, I.; Kolusheva, S.; Jelinek, R., Rapid colorimetric screening of drug interaction and penetration through lipid barriers. *Pharmaceutical research* **2006,** *23* (3), 580-588.
23. Ortuso, R. D.; Cataldi, U.; Sugihara, K., Mechanosensitivity of polydiacetylene with a

phosphocholine headgroup. *Soft Matter* **2017,** *13* (8), 1728-1736.
24. Nuck, J.; Sugihara, K., Mechanism of Polydiacetylene Blue-to-Red Transformation Induced by Antimicrobial Peptides. *Macromolecules* **2020,** *53* (15), 6469-6475.
25. Weston, M.; Tjandra, A. D.; Chandrawati, R., Tuning chromatic response, sensitivity, and specificity of polydiacetylene-based sensors. *Polymer Chemistry* **2020,** *11* (2), 166-183.
26. Lee, K. M.; Chen, X.; Fang, W.; Kim, J. M.; Yoon, J., A dual colorimetric and fluorometric sensor for lead ion based on conjugated polydiacetylenes. *Macromolecular rapid communications* **2011,** *32* (6), 497-500.
27. Wieprecht, T.; Seelig, J., Isothermal titration calorimetry for studying interactions between peptides and lipid membranes. In *Current Topics in Membranes*, Academic Press: 2002; Vol. 52, pp 31-56.
28. McLaughlin, S. G.; Szabo, G.; Eisenman, G., Divalent ions and the surface potential of charged phospholipid membranes. *J. Gen. Physiol.* **1971,** *58* (6), 667-87.
29. Abdulkader, F.; Arcisio-Miranda, M.; Curi, R.; Procopio, J., Surface potential determination in planar lipid bilayers: A simplification of the conductance-ratio method. *J. Biochem. Biophys. Methods* **2007,** *70* (3), 515-518.
30. Koivuniemi, A.; Fallarero, A.; Bunker, A., Insight into the antimicrobial mechanism of action of beta(2,2)-amino acid derivatives from molecular dynamics simulation: Dancing the can-can at the membrane surface. *Bba-Biomembranes* **2019,** *1861* (11).
31. Wei, M. L.; Liu, J. J.; Xia, Y. Y.; Feng, F.; Liu, W. Y.; Zheng, F., A polydiacetylene-based fluorescence assay for the measurement of lipid membrane affinity. *Rsc Adv* **2015,** *5* (81), 66420-66425.
32. Weiss, J. N., The Hill equation revisited: uses and misuses. *The FASEB Journal* **1997,** *11* (11), 835-841.
33. Abeliovich, H., An empirical extremum principle for the hill coefficient in ligand-protein interactions showing negative cooperativity. *Biophysical journal* **2005,** *89* (1), 76-79.
34. Hannestad, J. K.; Rocha, S.; Agnarsson, B.; Zhdanov, V. P.; Wittung-Stafshede, P.; Hook, F., Single-vesicle imaging reveals lipid-selective and stepwise membrane disruption by monomeric alpha-synuclein. *Proc. Natl. Acad. Sci. U. S. A.* **2020,** *117* (25), 14178-14186.
35. Huang, H. W., Molecular mechanism of antimicrobial peptides: The origin of cooperativity. *Biochimica et Biophysica Acta (BBA) - Biomembranes* **2006,** *1758* (9), 1292-1302.
36. Pabst, G.; Grage, S. L.; Danner-Pongratz, S.; Jing, W.; Ulrich, A. S.; Watts, A.; Lohner, K.; Hickel, A., Membrane thickening by the antimicrobial peptide PGLa. *Biophysical journal* **2008,** *95* (12), 5779-5788.
37. Kim, C.; Spano, J.; Park, E.-K.; Wi, S., Evidence of pores and thinned lipid bilayers induced in oriented lipid membranes interacting with the antimicrobial peptides, magainin-2 and aurein-3.3. *Biochimica et Biophysica Acta (BBA)-Biomembranes* **2009,** *1788* (7), 1482-1496.
38. Yang, L.; Harroun, T. A.; Weiss, T. M.; Ding, L.; Huang, H. W., Barrel-stave model or toroidal model? A case study on melittin pores. *Biophysical journal* **2001,** *81* (3), 1475-1485.
39. Park, S.-C.; Kim, J.-Y.; Shin, S.-O.; Jeong, C.-Y.; Kim, M.-H.; Shin, S. Y.; Cheong, G.-W.; Park, Y.; Hahm, K.-S., Investigation of toroidal pore and oligomerization by melittin using transmission electron microscopy. *Biochemical and biophysical research communications* **2006,** *343* (1), 222-228.
40. Vogel, H.; Jähnig, F., The structure of melittin in membranes. *Biophysical journal* **1986,** *50* (4), 573-582.
41. Naito, A.; Nagao, T.; Norisada, K.; Mizuno, T.; Tuzi, S.; Saitô, H., Conformation and dynamics of melittin bound to magnetically oriented lipid bilayers by solid-state 31P and 13C NMR spectroscopy. *Biophysical Journal* **2000,** *78* (5), 2405-2417.
42. Porcelli, F.; Verardi, R.; Shi, L.; Henzler-Wildman, K. A.; Ramamoorthy, A.; Veglia, G., NMR structure of the cathelicidin-derived human antimicrobial peptide LL-37 in dodecylphosphocholine micelles. *Biochemistry* **2008,** *47* (20), 5565-5572.
43. Oren, Z.; LERMAN, J. C.; GUDMUNDSSON, G. H.; AGERBERTH, B.; SHAI, Y., Structure and organization of the human antimicrobial peptide LL-37 in phospholipid membranes: relevance to the molecular basis for its non-cell-selective activity. *Biochemical Journal* **1999,** *341* (3), 501-513.

44. Sevcsik, E.; Pabst, G.; Richter, W.; Danner, S.; Amenitsch, H.; Lohner, K., Interaction of LL-37 with model membrane systems of different complexity: influence of the lipid matrix. *Biophysical journal* **2008,** *94* (12), 4688-4699.
45. Youngstrom, D. W.; Brender, J. R.; Smith, P. E.; Hartman, K.; Ramamoorthy, A., Formation of Toroidal Pores by Amyloid Proteins: Evidence of Lipid Transbilayer Exchange Induced by Islet Amyloid Polypeptide. *Biophysical Journal* **2010,** *98* (3), 458a.
46. Butterfield, S. M.; Lashuel, H. A., Amyloidogenic protein–membrane interactions: mechanistic insight from model systems. *Angewandte Chemie International Edition* **2010,** *49* (33), 5628-5654.
47. Smith, P. E.; Brender, J. R.; Ramamoorthy, A., Induction of negative curvature as a mechanism of cell toxicity by amyloidogenic peptides: the case of islet amyloid polypeptide. *Journal of the American Chemical Society* **2009,** *131* (12), 4470-4478.
48. Lipfert, J.; Columbus, L.; Chu, V. B.; Lesley, S. A.; Doniach, S., Size and shape of detergent micelles determined by small-angle X-ray scattering. *The journal of physical chemistry B* **2007,** *111* (43), 12427-12438.
49. Herrera, F. E.; Garay, A. S.; Rodrigues, D. E., Structural properties of CHAPS micelles, studied by molecular dynamics simulations. *The Journal of Physical Chemistry B* **2014,** *118* (14), 3912-3921.
50. Otten, D.; Löbbecke, L.; Beyer, K., Stages of the bilayer-micelle transition in the system phosphatidylcholine-C12E8 as studied by deuterium- and phosphorous-NMR, light scattering, and calorimetry. *Biophysical journal* **1995,** *68* (2), 584-597.
51. Matsuzaki, K.; Mitani, Y.; Akada, K.-y.; Murase, O.; Yoneyama, S.; Zasloff, M.; Miyajima, K., Mechanism of synergism between antimicrobial peptides magainin 2 and PGLa. *Biochemistry* **1998,** *37* (43), 15144-15153.
52. Last, N. B.; Miranker, A. D., Common mechanism unites membrane poration by amyloid and antimicrobial peptides. *Proc Natl Acad Sci U S A* **2013,** *110* (16), 6382-7.
53. Patel, H.; Huynh, Q.; Barlehner, D.; Heerklotz, H., Additive and synergistic membrane permeabilization by antimicrobial (lipo)peptides and detergents. *Biophys J* **2014,** *106* (10), 2115-25.
54. Drab, E.; Sugihara, K., Cooperative function of LL-37 and HNP1 protects mammalian cell membranes from lysis. *Biophysical journal* **2020,** *119* (12), 2440-2450.
55. Westerhoff, H. V.; Zasloff, M.; Rosner, J. L.; Hendler, R. W.; De Waal, A.; Vaz Gomes, A.; Jongsma, P. M.; Riethorst, A.; Juretic, D., Functional synergism of the magainins PGLa and magainin-2 in Escherichia coli, tumor cells and liposomes. *Eur. J. Biochem.* **1995,** *228* (2), 257-64.
56. Matsuzaki, K.; Mitani, Y.; Akada, K.; Murase, O.; Yoneyama, S.; Zasloff, M.; Miyajima, K., Mechanism of synergism between antimicrobial peptides magainin 2 and PGLa. *Biochemistry (Mosc).* **1998,** *37* (43), 15144-15153.
57. Kobayashi, S.; Hirakura, Y.; Matsuzaki, K., Bacteria-selective synergism between the antimicrobial peptides alpha-helical magainin 2 and cyclic beta-sheet tachyplesin I: toward cocktail therapy. *Biochemistry* **2001,** *40* (48), 14330-5.
58. Cirioni, O.; Silvestri, C.; Ghiselli, R.; Orlando, F.; Riva, A.; Mocchegiani, F.; Chiodi, L.; Castelletti, S.; Gabrielli, E.; Saba, V., *et al.*, Protective effects of the combination of alpha-helical antimicrobial peptides and rifampicin in three rat models of Pseudomonas aeruginosa infection. *J Antimicrob Chemother* **2008,** *62* (6), 1332-8.
59. Tang, Y. Q.; Yeaman, M. R.; Selsted, M. E., Antimicrobial peptides from human platelets. *Infect Immun* **2002,** *70* (12), 6524-33.
60. Yan, H.; Hancock, R. E., Synergistic interactions between mammalian antimicrobial defense peptides. *Antimicrob Agents Chemother* **2001,** *45* (5), 1558-60.
61. Levy, O.; Ooi, C. E.; Weiss, J.; Lehrer, R. I.; Elsbach, P., Individual and synergistic effects of rabbit granulocyte proteins on Escherichia coli. *J Clin Invest* **1994,** *94* (2), 672-82.
62. Rosenfeld, Y.; Barra, D.; Simmaco, M.; Shai, Y.; Mangoni, M. L., A synergism between temporins toward Gram-negative bacteria overcomes resistance imposed by the lipopolysaccharide protective layer. *J Biol Chem* **2006,** *281* (39), 28565-74.
63. Nuding, S.; Frasch, T.; Schaller, M.; Stange, E. F.; Zabel, L. T., Synergistic effects of antimicrobial peptides and antibiotics against Clostridium difficile. *Antimicrob Agents Chemother* **2014,** *58* (10), 5719-25.
64. Nagaoka, I.; Hirota, S.; Yomogida, S.; Ohwada, A.; Hirata, M., Synergistic actions of antibacterial

neutrophil defensins and cathelicidins. *Inflamm Res* **2000,** *49* (2), 73-9.

65. Luders, T.; Birkemo, G. A.; Fimland, G.; Nissen-Meyer, J.; Nes, I. F., Strong synergy between a eukaryotic antimicrobial peptide and bacteriocins from lactic acid bacteria. *Appl Environ Microbiol* **2003,** *69* (3), 1797-9.

66. Lauth, X.; Babon, J. J.; Stannard, J. A.; Singh, S.; Nizet, V.; Carlberg, J. M.; Ostland, V. E.; Pennington, M. W.; Norton, R. S.; Westerman, M. E., Bass hepcidin synthesis, solution structure, antimicrobial activities and synergism, and in vivo hepatic response to bacterial infections. *J. Biol. Chem.* **2005,** *280* (10), 9272-82.

67. Wang, Z. Y.; Zhang, L. C.; Wang, J.; Wei, D. D.; Shi, B. M.; Shan, A. S., Synergistic interaction of PMAP-36 and PRW4 with aminoglycoside antibiotics and their antibacterial mechanism. *World J Microb Biot* **2014,** *30* (12), 3121-3128.

68. Xiang, J.; Zhou, M.; Wu, Y. X.; Chen, T. B.; Shaw, C.; Wang, L., The synergistic antimicrobial effects of novel bombinin and bombinin H peptides from the skin secretion of Bombina orientalis. *Bioscience Rep* **2017,** *37*.

69. Zheng, Z. J.; Tharmalingam, N.; Liu, Q. Z.; Jayamani, E.; Kim, W.; Fuchs, B. B.; Zhang, R. J.; Vilcinskas, A.; Mylonakis, E., Synergistic Efficacy of Aedes aegypti Antimicrobial Peptide Cecropin A2 and Tetracycline against Pseudomonas aeruginosa. *Antimicrob Agents Ch* **2017,** *61* (7).

70. Marxer, M.; Vollenweider, V.; Schmid-Hempel, P., Insect antimicrobial peptides act synergistically to inhibit a trypanosome parasite. *Philos T R Soc B* **2016,** *371* (1695).

71. Svensson, D.; Lagerstedt, J. O.; Nilsson, B. O.; Del Giudice, R., Apolipoprotein A-I attenuates LL-37-induced endothelial cell cytotoxicity. *Biochem Bioph Res Co* **2017,** *493* (1), 71-76.

72. Yang, A.; Wang, C.; Song, B.; Zhang, W.; Guo, Y.; Yang, R.; Nie, G.; Yang, Y.; Wang, C., Attenuation of beta-Amyloid Toxicity In Vitro and In Vivo by Accelerated Aggregation. *Neurosci Bull* **2017,** *33* (4), 405-412.

73. De Lorenzi, E.; Chiari, M.; Colombo, R.; Cretich, M.; Sola, L.; Vanna, R.; Gagni, P.; Bisceglia, F.; Morasso, C.; Lin, J. S., *et al.*, Evidence that the Human Innate Immune Peptide LL-37 may be a Binding Partner of Amyloid-beta and Inhibitor of Fibril Assembly. *J Alzheimers Dis* **2017,** *59* (4), 1213-1226.

74. Williams, R. W.; Starman, R.; Taylor, K. M. P.; Gable, K.; Beeler, T.; Zasloff, M.; Covell, D., Raman-Spectroscopy of Synthetic Antimicrobial Frog Peptides Magainin-2a and Pgla. *Biochemistry (Mosc).* **1990,** *29* (18), 4490-4496.

75. Tremouilhac, P.; Strandberg, E.; Wadhwani, P.; Ulrich, A. S., Synergistic transmembrane alignment of the antimicrobial heterodimer PGLa/magainin. *J. Biol. Chem.* **2006,** *281* (43), 32089-32094.

76. Salnikov, E. S.; Bechinger, B., Lipid-Controlled Peptide Topology and Interactions in Bilayers: Structural Insights into the Synergistic Enhancement of the Antimicrobial Activities of PGLa and Magainin 2. *Biophys. J.* **2011,** *100* (6), 1473-1480.

77. Nishida, M.; Imura, Y.; Yamamoto, M.; Kobayashi, S.; Yano, Y.; Matsuzaki, K., Interaction of a magainin-PGLa hybrid peptide with membranes: Insight into the mechanism of synergism. *Biochemistry (Mosc).* **2007,** *46* (49), 14284-14290.

78. Zerweck, J.; Strandberg, E.; Kukharenko, O.; Reichert, J.; Burck, J.; Wadhwani, P.; Ulrich, A. S., Molecular mechanism of synergy between the antimicrobial peptides PGLa and magainin 2. *Sci Rep-Uk* **2017,** *7*.

79. Han, E.; Lee, H., Synergistic effects of magainin 2 and PGLa on their heterodimer formation, aggregation, and insertion into the bilayer. *Rsc Adv* **2015,** *5* (3), 2047-2055.

80. Tallarida, R. J., Quantitative methods for assessing drug synergism. *Genes Cancer* **2011,** *2* (11), 1003-8.

81. Foucquier, J.; Guedj, M., Analysis of drug combinations: current methodological landscape. *Pharmacol Res Perspect* **2015,** *3* (3), e00149.

TOC graphic

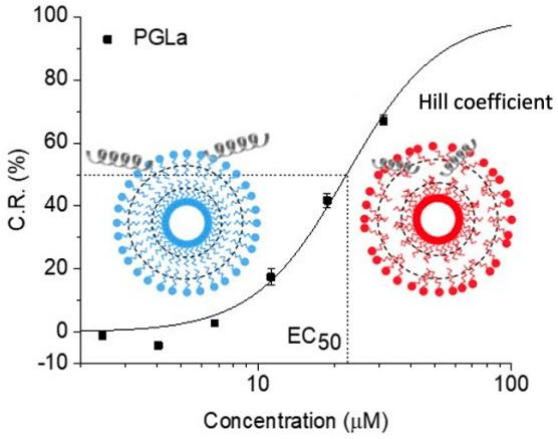
PGLa
Hill coefficient
C.R. (%)
EC50
Concentration (μM)
100
80
60
40
20
0
-10
10
100